Modeling the circulation of the intermediate layer in the Sea of Okhotsk

Keisuke Uchimoto, Tomohiro Nakamura, Jun Nishioka and Humio Mitsudera

Institute of Low Temperature Science, Hokkaido University, Sapporo, Japan
E-mail: uchimoto@lowtem.hokudai.ac.jp

Introduction

Recently, the Sea of Okhotsk has been recognized as a primary iron source region to the northwestern Pacific (Nishioka *et al.*, 2007). Cold and dense water, which is referred to as Dense Shelf Water (DSW), is formed as a result of brine rejection from sea ice on the northwestern shelf in the Sea of Okhotsk. Iron, together with other chemical particles, is considered to be incorporated into DSW through, for example, tidal mixing (Nakatsuka *et al.*, 2004). DSW, including iron, is transported southward by the East Sakhalin Current in the intermediate layer off Sakhalin, and flows out into the Pacific through the Kuril straits. Thus iron is supplied to the northwestern Pacific.

We intend to model the iron circulation and distribution from the Sea of Okhotsk to the northeastern Pacific in the near future. We have constructed an Ocean General Circulation Model (OGCM) on which we will overlay an iron model. In this paper, we describe the OGCM and show some results of the OGCM, with the above picture of iron circulation in mind. Then, we show tracer experiments in which a tracer is injected in winter at the sea surface in the northwestern part of the Sea of Okhotsk to trace DSW in the model.

OGCM

The model used is Iced COCO ver. 3.4 (Hasumi *et al.*, 2004). It is the ice–ocean coupled model developed at the center for Climate System Research, University of Tokyo. In the ocean model, the vertical coordinate system is a hybrid of sigma (between the sea surface and a depth of 31 m) and z level coordinate (below 31 m). The partial step formulation is adopted for bottom topography (Adcroft *et al.*, 1997). For the tracer equations, the advection schemes are the Quadratic Upstream Interpolation for Convective Kinematics with Estimate Streaming Terms (Leonard, 1979) and the Uniformly Third-Order Polynominal Interpolation Algorithm (Leonard *et al.*, 1993), and isopycnal diffusion (Cox, 1987), thickness diffusion (Gent *et al.*, 1995), and the turbulence closure of Noh and Kim (1999) are used. The isopycnal and the thickness diffusion coefficients are 1.0×10^6 cm^2/s and 3.0×10^6 cm^2/s, respectively, and the background vertical viscosity and diffusion coefficients are 1.0 cm^2/s and 0.1 cm^2/s, respectively. In the ice model, the thermodynamic part is the zero layer model (Semtner, 1976), and the dynamic part is the elastic-viscous-plastic formulation of Hunke and Dukowicz (1997) with two-category thickness representation.

The model domain spans from 136°E to 179.5°W and from 39°N to 63.5°N. The horizontal resolution is 0.5° both in zonal and meridional directions. There are 51 levels in the vertical direction with thickness increasing from 1 m at the sea surface to 1000 m in the deepest layer.

The OGCM is forced at the sea surface by the daily mean climatology data set (wind stress, freshwater flux, radiation, wind speed, temperature, and humidity) from the Ocean Model Intercomparison Project. The freshwater flux data consist of evaporation, precipitation, and river runoff. While the freshwater flux is much larger at the northern mouth of the Mamiya (Tartar) Strait than its vicinities throughout the year, probably owing to the runoff from the Amur River, the runoff ought to drop or stop in winter because of freezing of the river. Therefore, we subtract the annual mean (which we regard as approximate river runoff) from the data at each grid the north of 53°N and the west of 142°E in winter (from December 15 to April 15) and the amount of the subtraction is evenly distributed to the rest of the days.

Temperature and salinity are restored to the World Ocean Atlas data (WOA) on the 6 grids from the boundaries, and the sea surface height is restored to the basin-wide model outputs on the 3 grids from the boundaries. Temperature and salinity are also restored to the WOA at grids deeper than 2000 m. The sea surface salinity (SSS) is restored to the WOA. From December to April, the SSS is not restored to the WOA in the northern half of the Sea of Okhotsk, as the SSS around the northwestern part of the Sea of Okhotsk in the WOA is too low in winter probably owing to the spurious effects of the Amur River runoff.

Although circulations in and around the Sea of Okhotsk are strongly affected by tidal mixing along the Kuril Islands, this OGCM does not include tidal effects. Therefore, we increased the vertical diffusion coefficients as tidal effects along the Kuril Islands, where the coefficients are set at 500 cm^2/s at the bottom and decrease upward.

The OGCM is integrated for 116 years from the rest with the climatological temperature and salinity (WOA). The next section describes monthly means of the results in the last 1 year.

Results

Figure 1 shows barotropic streamlines in winter and summer. There is a cyclonic gyre in the center of the Sea of Okhotsk, which is strong in winter and weak in summer. In summer, in the southern part of the Sea near the Kuril Islands, the values are positive and some anticyclonic circulations are seen. These circulations and their seasonal variations are consistent with previous studies (*e.g.*, Ohshima *et al.*, 2004; Uchimoto *et al.*, 2007).

Figure 2 shows an ice concentration map in February. This shape of ice distribution is very similar to satellite observations (*e.g.*, Ohshima *et al.*, 2006). We should note that the concentration is somewhat low (less than 0.95) along the northern and northwestern coast. This low concentration is thought to be due to coastal polynyas, where sea ice is mainly produced and therefore much brine is rejected. This implies that DSW is produced in the OGCM.

Next, some features on and about the $26.8\sigma_\theta$ surface are shown. The $26.8\sigma_\theta$ surface is a typical surface in the intermediate layer. Figure 3 shows the depth. Although the model result is somewhat shallower than the climatology (Itoh *et al.*, 2003) almost everywhere in the Sea of Okhotsk, the model result has a general resemblance to the climatology. One of the salient features in the climatology is a deep zone (~300 m) in the Kuril Basin. In the OGCM, the deep zone is marginally represented; the area is smaller and the depth is shallower (~200 m). Another salient feature in the climatology is a deep region in the southeastern part of the Sea of Okhotsk. The deep region is represented in the OGCM, and it extends toward the northwest, the same as in the climatology.

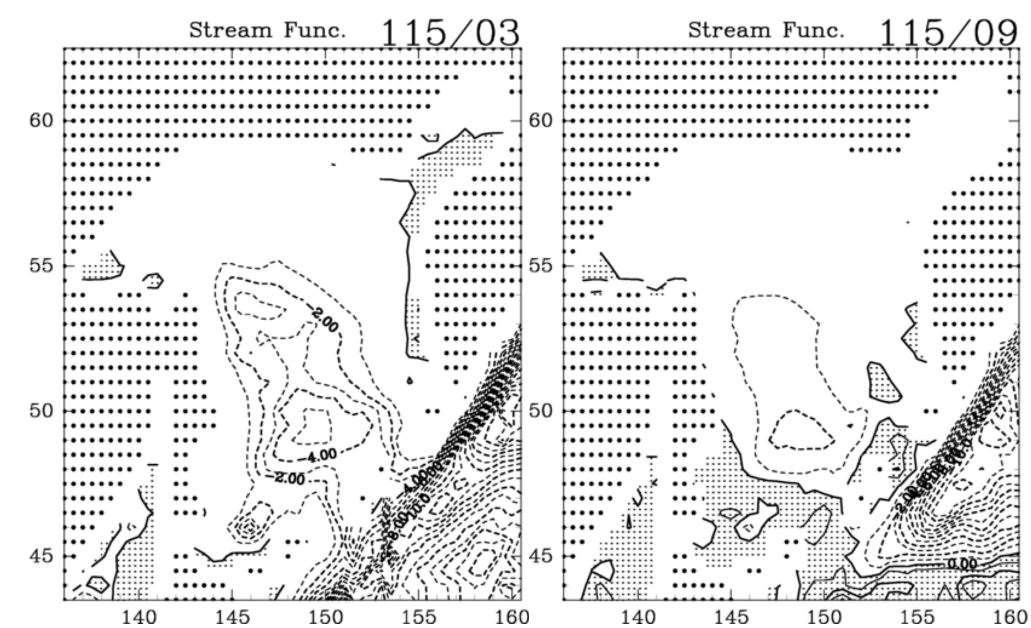

Fig. 1 Barotropic streamlines in March (left) and September (right). Shaded region denotes positive values of streamlines. Contour interval is 1 Sv.

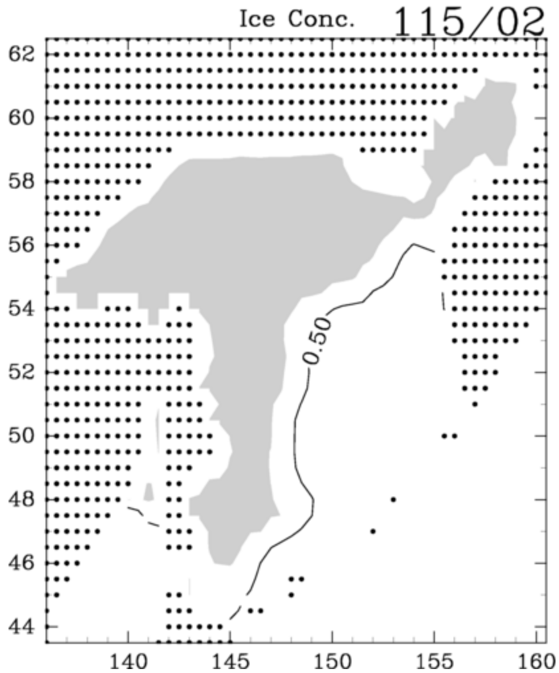

Fig. 2 Ice concentration map in February. Shaded region is where the concentration is larger than 0.95. The contour denotes concentration of 0.5.

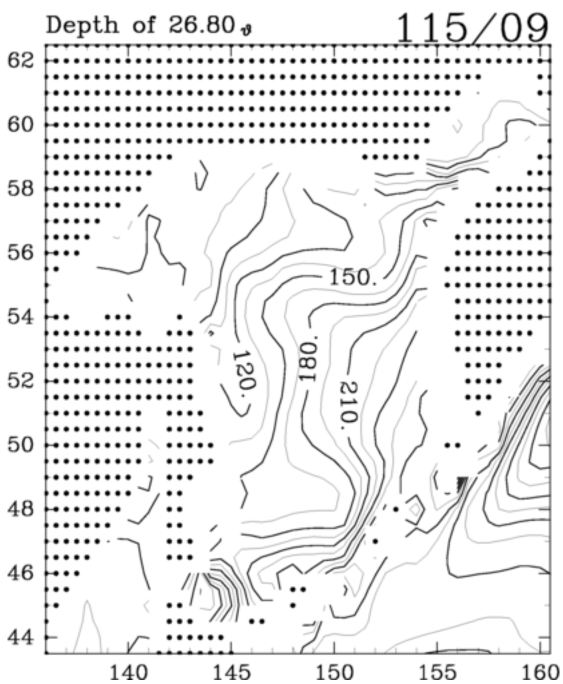

Fig. 3 Depth of the 26.8 σ_θ surface in September. Contour interval is 15 m.

The 26.8σ_θ surface in the OGCM outcrops in winter around the northwestern shelf (not shown). Cold water extends southward from the shelf along Sakhalin Island (Fig. 4). In the center and eastern part of the Sea, potential temperature is relatively high because warm water from the Pacific enters the Sea of Okhotsk. Temperature there is slightly higher, by about 0.8°C, in the OGCM than in the climatology.

The thickness of the 26.8σ_θ layer that is defined as the distance between the two surfaces of 26.75σ_θ and 26.85σ_θ is shown in Figure 5. The thick layer in the eastern part of the Sea is represented in the OGCM, but the thick layer in the southern part is, unfortunately, not represented.

In summary, the OGCM represents circulations and features of the 26.8σ_θ in the Sea of Okhotsk, of course not perfectly, but acceptably well, considering its coarse resolution. The area most poorly represented in the OGCM is the Kuril Basin. While the cause for it is not apparent at present, a possible cause is the parameterization of tidal mixing effects along the Kuril Islands. We should investigate more appropriate values and/or vertical profiles of the vertical diffusion coefficients using tidal mixing effects.

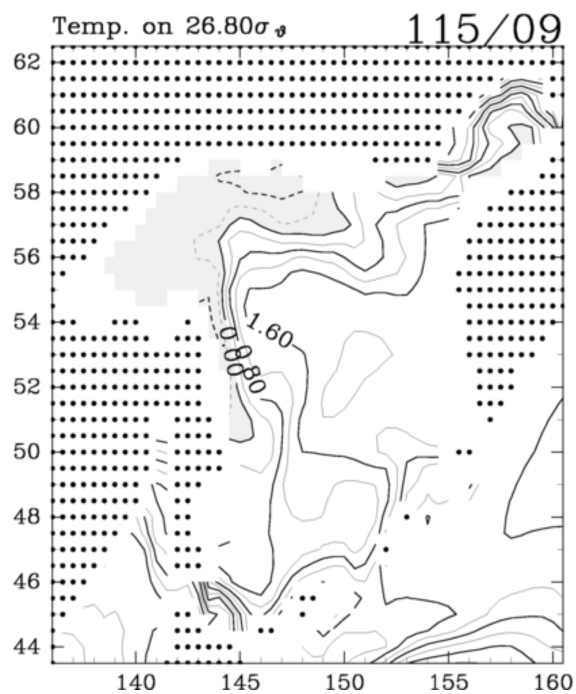

Fig. 4 Temperature on the 26.8σ_θ surface in September. Contour interval is 0.4°C. Regions where temperature is less than 0°C are shaded.

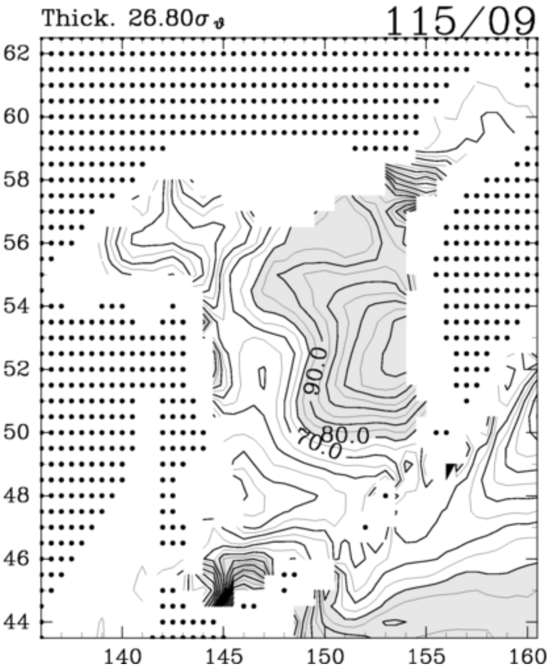

Fig. 5 Thickness of the 26.8σ_θ surface in September. Contour interval is 5 m. Regions where the thickness is larger than 80 m are shaded.

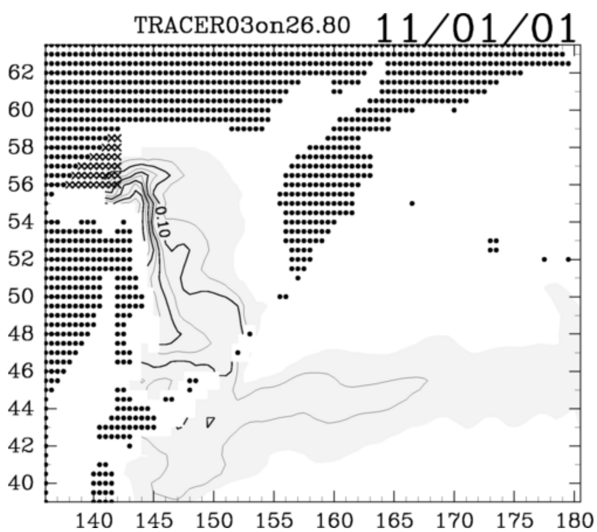

Fig. 6 Tracer concentration on the 26.8σ_θ surface 11 years after the start. The tracer injected from January to April at the sea surface in the northwestern shelf is denoted by crosses. Contour interval is 0.05. Regions where tracer concentration is larger than 0.1 are shaded.

Tracer experiments

To trace dense water that is produced as a result of cooling and brine rejection around the northwestern shelf, we conducted tracer experiments, where a passive tracer is restored to unity at the sea surface in the northwestern shelf (Fig. 6) from January to April.

Figure 6 displays tracer distribution on the 26.8σ_θ surface 11 years after the start. The tracer injected near the northwestern corner of the Sea moves southward along the western coast on the shelf and then eastward around 55°N. It moves southward along Sakhalin Island and goes toward the Kuril Islands. Some part of the tracer recirculates within the Sea of Okhotsk, and the other parts move into the Pacific through the Kuril Straits where they are transported eastward in the North Pacific.

Along 55°N the tracer leaves the shelf and proceeds on the slope. At first, the tracer appears in the vertical section along 55°N, with a stronger concentration near the bottom in the western part, creeps eastward, and then goes down the slope. However, it does not reach the bottom on the slope, but remains in the intermediate layer. This picture is consistent with observed DSW which is produced on the northwestern shelf and is transported in the intermediate layer, in a depth of a few hundreds meters.

We also conducted the same experiment but with *no* tidal mixing effects along the Kuril Islands. In the no mixing case, the tracer does not sink to the intermediate layer on the slope, but remains at almost the same depth as the shelf bottom (not shown). The difference between the two cases indicates that tidal mixing along the Kuril Islands indirectly pushes DSW to a depth of a few hundred meters, *i.e.*, the intermediate layer.

Concluding Remarks

We have shown some results of our OGCM which covers the Sea of Okhotsk and the northwestern Pacific. Considering its coarse resolution, we think that the OGCM can represent circulations and active tracer distributions in the intermediate layer well. Tracer experiments show that dense and cold water (DSW) produced on the northwestern shelf in the Sea of Okhotsk flows southward along Sakhalin in the intermediate layer.

We will overlay an iron model on the OGCM and investigate the iron circulation. Since iron is thought to be transported with DSW, the results suggest that the OGCM is likely to be useful for iron circulation modeling.

References

Adcroft, A., Hill, C. and Marshall, J. 1997. Representation of topography by shaved cells in a height coordinate ocean model. *Mon. Wea. Rev.* **125**: 2293–2315.

Cox, M.D. 1987. Isopycnal diffusion in a z-coordinate ocean model. *Ocean Modelling* **74**: 1–5.

Gent, P.R., Willebrand, J., McDougall, T.J. and McWilliams, J.C. 1995. Parameterizing eddy induced tracer transports in ocean circulation models. *J. Phys. Oceanogr*. **25**: 463–474.

Hasumi, H., Oka, A. and Komuro, Y. 2004. A study on the polar ocean freshwater budget and the global thermohaline circulation using the CCSR sea ice-ocean model (Iced-COCO). CGER's Supercomputure Activity Report, 11-2002, pp. 11–20.

Hunke, E.C. and Dukowicz, J.K. 1997. An elastic-viscous-plastic model for sea ice dynamics. *J. Phys. Oceanogr*. **27**: 1849–1867

Itoh, M., Ohshima, K.I. and Wakatsuchi, M. 2003. Distribution and formation of Okhotsk Sea Intermediate Water: An analysis of isopycnal climatological data. *J. Geophys. Res*. **108**: doi:10.1029/2002JC001590

Leonard, B.P. 1979. A stable and accurate convective modelling procedure based on quadratic upstream interpolation. *Comput. Method Appl. Mech. Eng.* **19**: 59–98.

Leonard, B.P., MacVean, M.K. and Lock, A.P. 1993. Positivity-preserving numerical schemes for multidimensional advection. NASA Tech. Memo. 106055, ICOMP-93-05.

Nakatsuka, T., Fujimune, T., Yoshikawa, C., Noriki, S., Kawamura, K., Fukamachi, Y., Mizuta, G. and Wakatsuchi, M. 2004. Biogenic and lithogenic particle fluxes in the western region of the Sea of Okhotsk: Implications for lateral material transport and biological productibity. *J. Geophys. Res.* **109**: C09S13: doi:10.1029/2003JC001908

Nishioka, J., Ono, T., Saito, H., Nakatsuka, T., Takeda, S., Yoshimura, T. Suzuki, K., Kuma, K., Nakabayashi, S., Tsumune, D., Mitsudera, H., Johnson, W.K. and Tsuda, A. 2007. Iron supply to the western subarctic Pacific: Importance of iron export from the Sea of Okhotsk. *J. Geophys. Res.* **112**: C10012: doi:10.1029/2006JC04055

Noh, Y. and Kim, J. 1999. Simulations of temperature and turbulence structure of the oceanic boundary layer with the improved near-surface process. *J. Geophy. Res.* **104**: 15,621–15,634.

Ohshima, K.I., Simizu, D., Itoh, M., Mizuta G., Fukamachi, Y., Riser, S.C. and Wakatsuchi, M. 2004. Sverdrup balance and the cyclonic gyre in the Sea of Okhotsk. *J. Phys. Oceanogr.* **34**: 513–525.

Ohshima, K.I., Nihashi, S., Hashiya, E. and Watanabe, T. 2006. Interannual variability of sea ice area in the Sea of Okhotsk: Importance of surface heat flux in fall. *J. Meteor. Soc. Japan* **84**: 907–919.

Semtner, A.J., Jr. 1976. A model for the thermo-dynamic growth of sea ice in numerical investigations of climate. *J. Phys. Oceanogr.* **6**: 379–389

Uchimoto, K., Mitsudera, H., Ebuchi, N. and Miyazawa, Y. 2007. Anticyclonic eddy caused by the Soya Warm Current in an Okhotsk OGCM. *J. Oceanogr.* **63**: 379–391.